Ultrafast Nuclear Dynamics in Methylamine in Few-cycle Laser Field

(University of Tokyo, School of Science)
○Meng Zhang, Toshiaki Ando, Atsushi Iwasaki, Kaoru Yamanouchi

Introduction

It has been revealed from our recent studies that ultrafast hydrogen migration proceeds in hydrocarbon molecules when they are irradiated with ultrashort intense laser pulses [1, 2]. In the present study, hydrogen migration processes of methylamine induced by few-cycle intense near-infrared pulses were investigated by the coincidence momentum imaging (CMI) method. By the analysis of the released kinetic energy distributions of the Coulomb explosion pathways:

$$CH_3NH_2^{2+} \rightarrow CH_3^+ + NH_2^+ \quad \textit{(non-hydrogen migration pathway)}, \qquad (1)$$
$$CH_3NH_2^{2+} \rightarrow CH_2^+ + NH_3^+ \quad \textit{(hydrogen migration pathway)}, \qquad (2)$$

we found that there are two peaks in the angle-resolved released kinetic energy distribution in the hydrogen migration pathway, indicating that two different electronic states are involved both in the hydrogen migration and in the non-migration pathways.

Experimental

The output of a chirped-pulse-amplification femtosecond Ti:sapphire laser system (0.5 mJ, 30 fs, 5 kHz, 800 nm) was focused into a hollow-core fiber (1.5 m in length, 300 μm in inner diameter) filled with an Ar gas (0.5 atm) and the spectrum was broadened through the self-phase-modulation. The spectral phase dispersion was compensated by chirped mirrors and wedged fused silica plates. The pulse duration was measured by a two-dimensional spectral interferometer to be 4.3 fs. The few-cycle laser pulses were introduced to an ultrahigh vacuum chamber for ion momentum imaging and focused by a concave mirror ($f = 150$ mm) on a molecular beam of methylamine. The laser field intensity at the focal spot was estimated to be 1.3×10^{14} W/cm^2 from the pulse energy, pulse duration and focal spot size. The parent and fragment ions were guided by a static electric field in the velocity map configuration toward a position sensitive detector with delay-line anodes (HEX120, RoentDek). The count rate of the fragment ions was 2×10^3 cps. The momentum vectors of the fragment ions were determined from the flight time and the positions of the fragment ions. By applying coincidence momentum conditions, the Coulomb explosion pathways (1) and (2) were extracted.

Result and Discussion

Figure 1(a) and (b) shows the distribution of the released kinetic energy E_{kin} in the Coulomb explosion pathway: non-migration ($CH_3NH_2^{2+} \rightarrow CH_3^+ + NH_2^+$) and migration ($CH_3NH_2^{2+} \rightarrow CH_2^+ + NH_3^+$) pathways. In the hydrogen migration pathway, we found two peaks at 4.1 eV and 5.6 eV. In the non-migration pathway, we found only one peak at 5.5 eV with a shoulder structure. The two peaks appearing in the hydrogen migration means that the precursor species for the hydrogen migration pathways are prepared in the two different electronic states from which the Coulomb explosion process (2) proceeds.

Figures 1(c) and (d) show the angle-resolved kinetic energy distributions $I(E_{kin}, \theta) = Y(E_{kin}, \theta)/\sin\theta$, where the θ is the angle of the momentum of the fragment ions with respect to the laser polarization direction and Y is the ion yields. In the non-migration pathway, the distribution exhibits maxima at around $\pi/4$ and $3\pi/4$ radiands at 6.9 eV while the distribution of the fragment ions are stretched along the laser polarization direction at 5.8 eV. These angular distributions can be ascribed to the angle dependent ionization probability of CH_3NH_2, and the different angular distributions at 5.8 eV and 6.9 eV indicate that $CH_3NH_2^{2+}$ is prepared by the ejection of the electrons from different molecular orbitals. In the migration pathway, the angular distribution of the lower E_{kin}

component at 3.7-5.0 eV exhibits a flat angular dependence, and that of the higher E_{kin} component at 5.0-7.5 eV exhibits peaks at around 0.5 radians and 2.6 radiands. From the angle resolved kinetic energy distributions, it is shown that these pathways are originated from the two different precursor states.
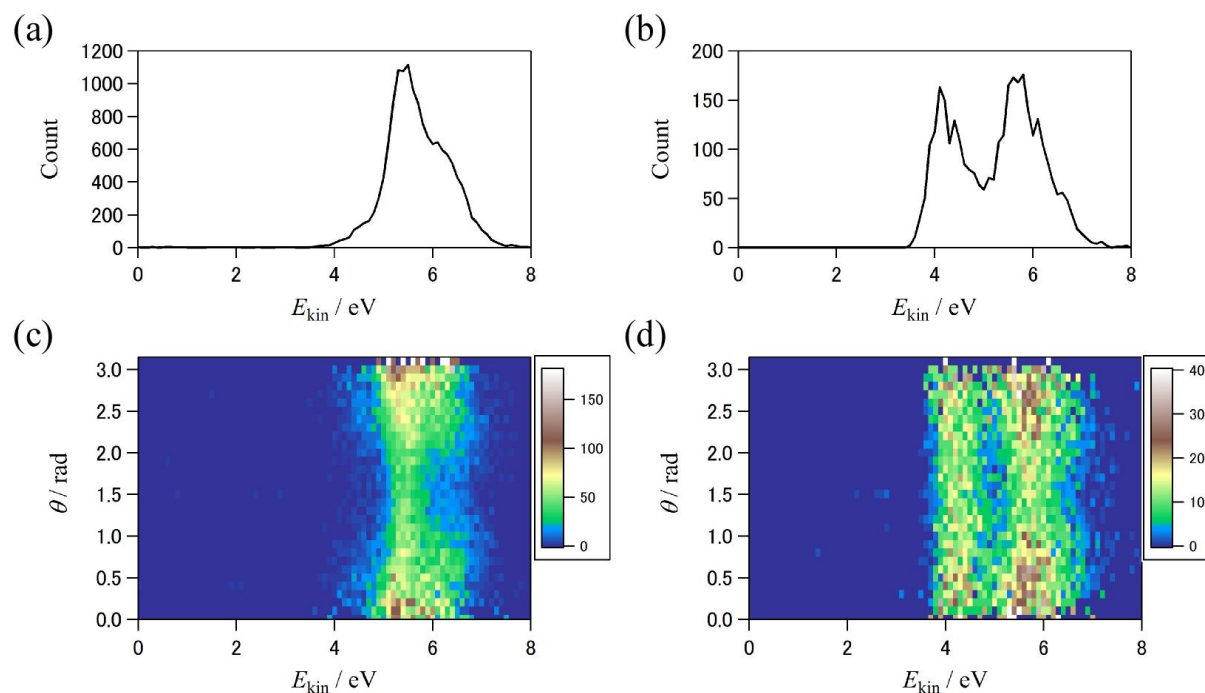

Figure1. The distributions of the released kinetic energy E_{kin} in (a) the non-migration pathway ($CH_3NH_2^{2+} \rightarrow CH_3^+ + NH_2^+$) and (b) the migration pathway ($CH_3NH_2^{2+} \rightarrow CH_2^+ + NH_3^+$). The angle-resolved kinetic energy distributions for (c) the non-migration pathway and (d) the migration pathway.

References:
[1] A. Hishikawa, H. Hasegawa, K. Yamanouchi, *J. Electr. Spectr. Rel. Phenom.* **141**, 195 (2004).
[2] T. Ando, A. Shimamoto, S. Miura, K. Nakai, H. Xu, A. Iwasaki, K. Yamanouchi, *Chem. Phys. Lett.* **624**, 78 (2015).